Hydrogeol J (2016) 24:1359–1373
DOI 10.1007/s10040-016-1408-9

REPORT

Groundwater flow dynamics of weathered hard-rock aquifers under climate-change conditions: an illustrative example of numerical modeling through the equivalent porous media approach in the north-western Pyrenees (France)

J. Jaunat[1] · A. Dupuy[2] · F. Huneau[3,4] · H. Celle-Jeanton[5] · P. Le Coustumer[2,6,7]

Received: 25 September 2015 / Accepted: 22 March 2016 / Published online: 6 April 2016

Abstract A numerical groundwater model of the weathered crystalline aquifer of Ursuya (a major water source for the north-western Pyrenees region, south-western France) has been computed based on monitoring of hydrological, hydrodynamic and meteorological parameters over 3 years. The equivalent porous media model was used to simulate groundwater flow in the different layers of the weathered profile: from surface to depth, the weathered layer ($5 \cdot 10^{-8} \leq K \leq 5 \cdot 10^{-7}$ m s^{-1}), the transition layer ($7 \cdot 10^{-8} \leq K \leq 1 \cdot 10^{-5}$ m s^{-1}, the highest values being along major discontinuities), two fissured layers ($3.5 \cdot 10^{-8} \leq K \leq 5 \cdot 10^{-4}$ m s^{-1}, depending on weathering profile conditions and on the existence of active fractures), and the hard-rock basement simulated with a negligible hydraulic conductivity ($K = 1\ 10^{-9}$). Hydrodynamic properties of these five calculation layers demonstrate both the impact of the weathering degree and of the discontinuities on the groundwater flow. The great agreement between simulated and observed hydraulic conditions allowed for validation of the methodology and its proposed use for application on analogous aquifers. With the aim of long-term management of this strategic aquifer, the model was then used to evaluate the impact of climate change on the groundwater resource. The simulations performed according to the most pessimistic climatic scenario until 2050 show a low sensitivity of the aquifer. The decreasing trend of the natural discharge is estimated at about −360 m^3 y^{-1} for recharge decreasing at about −5.6 mm y^{-1} (0.8 % of annual recharge).

Keywords Fracture rocks · Numerical modeling · Climate change · Equivalent porous media · France

Introduction

Water resources (surface water and groundwater) are directly affected by global warming. The temporal and spatial evolutions of the hydrological cycle induced by climate change are largely documented (e.g. Brouyère et al. 2004; Kumar 2012;

Electronic supplementary material The online version of this article (doi:10.1007/s10040-016-1408-9) contains supplementary material, which is available to authorized users.

✉ J. Jaunat
jessy.jaunat@univ-reims.fr

[1] Université de Reims Champagne-Ardenne, EA 3795 – GEGENAA, 2 esplanade Roland Garros, F-51100 Reims, France

[2] Bordeaux INP, EA 4592 Géoressources & Environnement, ENSEGID, 1 allée F. Daguin, 33607 Pessac Cedex, France

[3] Université de Corse Pascal Paoli, Laboratoire d'Hydrogéologie, Campus Grimaldi, BP 52, F-20250 Corte, France

[4] CNRS, UMR 6134 SPE, BP 52, F-20250 Corte, France

[5] CNRS, UMR 6249 Chrono-Environnement, Université de Franche-Comté, 16 route de Gray, F-25000 Besançon, France

[6] Université de Bordeaux, UF ST, B.18, Av G. Saint-Hilaire, 33615 Pessac Cédex, France

[7] Université de Pau et pays de l'Adour, UMR-CNRS 5254 IPREM, Technopole Hélioparc, 2 av. P. Angot, 64053 Pau Cedex 09, France

Neukum and Azzam 2012; Zhou et al. 2010). Many scientific studies have been carried out focusing on surface-water systems (Treidel et al. 2012), but before 2010 only a few studies discussed the evolution of groundwater resources in the next decades (e.g. Aguilera and Murillo 2009; Bloomfield et al. 2003; Bouraoui et al. 1999; Eckhardt and Ulbrich 2003). However, the impact of climate variations on groundwater resources is an important aspect for future water management (Taylor et al. 2012). Nowadays, this topic is handled more frequently in the literature (e.g. Allen et al. 2010; Virdi et al. 2013; Bertrand et al. 2014; Klove et al. 2014; Landes et al. 2014), especially on the theme of models for forecasting groundwater flow for efficient groundwater management (e.g. Mahmoodzadeh et al. 2014; Molina et al. 2013; Shamir et al. 2015).

The study described here deals with this topic in the specific hydrogeological context of fractured-rock aquifers. The materials of the study area are characterized by a high degree of weathering, and can be considered as an interesting hard rock aquifer comparable to those developed in tropical and sub-tropical areas where groundwater modeling is poorly documented (e.g. Australia, Banks et al. 2009; Malawi, Chilton and Smith-Carington 1984; Burkina Faso, Courtois et al. 2010; India, Dewandel et al. 2006; Central African Republic, Djebebe-Ndjiguim et al. 2013). Fractured-rock environments are an important field of study due to their abundance and increasing uses for water supply worldwide (Ayraud et al. 2008; Bertrand et al. 2010; Glynn and Plummer 2005; Berkowitz 2002).

Different approaches exist to model groundwater flow in discontinuous aquifers. The 'equivalent porous media' approach has been used in this study (e.g. Abusaada and Sauter 2013; Boronina et al. 2003; Carrera et al. 1990; Davison 1985; Hsieh and Neuman 1985). Here, the primary and secondary porosity and the hydraulic conductivity distribution are replaced by a continuous porous medium having equivalent hydraulic properties (Cook 2003).

The modeling strategy described in this report is applied to the gneissic aquifer of the Ursuya massif, in a specific geological context of hard rock aquifers exhibiting a high degree of weathering. The weathering profile developed in hard rock aquifers is of primary importance for flow conditions in such media (Ayraud et al. 2008; Dewandel et al. 2006; Hrkal et al. 2009; Jaunat et al. 2012; Wyns et al. 2004). Indeed, numerous studies highlight that the degree of weathering is one of the major parameters constraining the groundwater flows in hard rock media (Koïta et al. 2013; Lachassagne et al. 2011). The first aim of the study is to assess the impact of this weathering profile and of the geological discontinuities on groundwater flows by the use of numerical modelling tools. The study also aims to assess the impact of the regional projected climate conditions on the local groundwater resources since the study site is one of the main drinking-water-supply resources of the north-western Pyrenees region.

The differential groundwater flowpaths of this system have been previously defined according to geochemical and isotopic investigations on groundwater and recharge waters (Jaunat et al. 2012, 2013). These results, with a significant database of 3 years, and with the monitoring of runoff, hydraulic head and climate parameters, allowed the establishment of a groundwater flow model in finite elements. Long-term predictive simulations were then performed (up to 2050) to estimate the potential evolution of the groundwater resources in relation to climate change.

General setting

Geological situation

Located in the north-western Pyrenees (south-western France), 25 km from Bayonne city and from the Atlantic coast, the Ursuya Massif is the first relief of the north-western part of the Pyrenees coming from the north. The Ursuya Mount is constituted of Precambrian crystalline metamorphic formations (basic gneisses and pargneisses; Boissonnas et al. 1974) distributed between the Nive River bed—at 40 m above sea level (ASL) and 678 mASL (Ursuya Mount, Fig. 1a). Thin sections of metamorphosed limestone have also been observed in some boreholes (Armand et al. 1995; Boissonnas et al. 1974) but their distribution is poorly defined. It is the same for some pegmatite lenses (Ondarroa et al. 1998).

These Precambrian crystalline formations are strongly fractured and show a high density of lineaments (Fig. 1b, Boissonnas et al. 1974; Jaunat 2012) mainly attributed to the Hercynian tectonic but also to a post-Hercynian evolution (Engeser and Schwentke 1986; Feuillée and Rat 1971; Larrasoaña et al. 2003; Turner 1996). The map of lineaments shows a NW–SE major orientation, which is in agreement with the geological context of the Pyrenees (e.g. Mattauer and Henry 1974).

The study site (Fig. 1a) is composed of an important layer of weathered material (frequently more than 10 m thick) covering a fissured layer. The transition between these two layers is gradual with an increasing weathering from the fissured to the weathered layer. This lithology is typical of crystalline aquifer profiles with three superimposed layers (from surface to depth: weathered, transition and fissured) when the profile is completely preserved (Chilton and Smith-Carington 1984; Chilton and Foster 1995; Courtois et al. 2010; Dewandel et al. 2006; Hrkal et al. 2009; Lachassagne et al. 2011; Wyns et al. 2004).

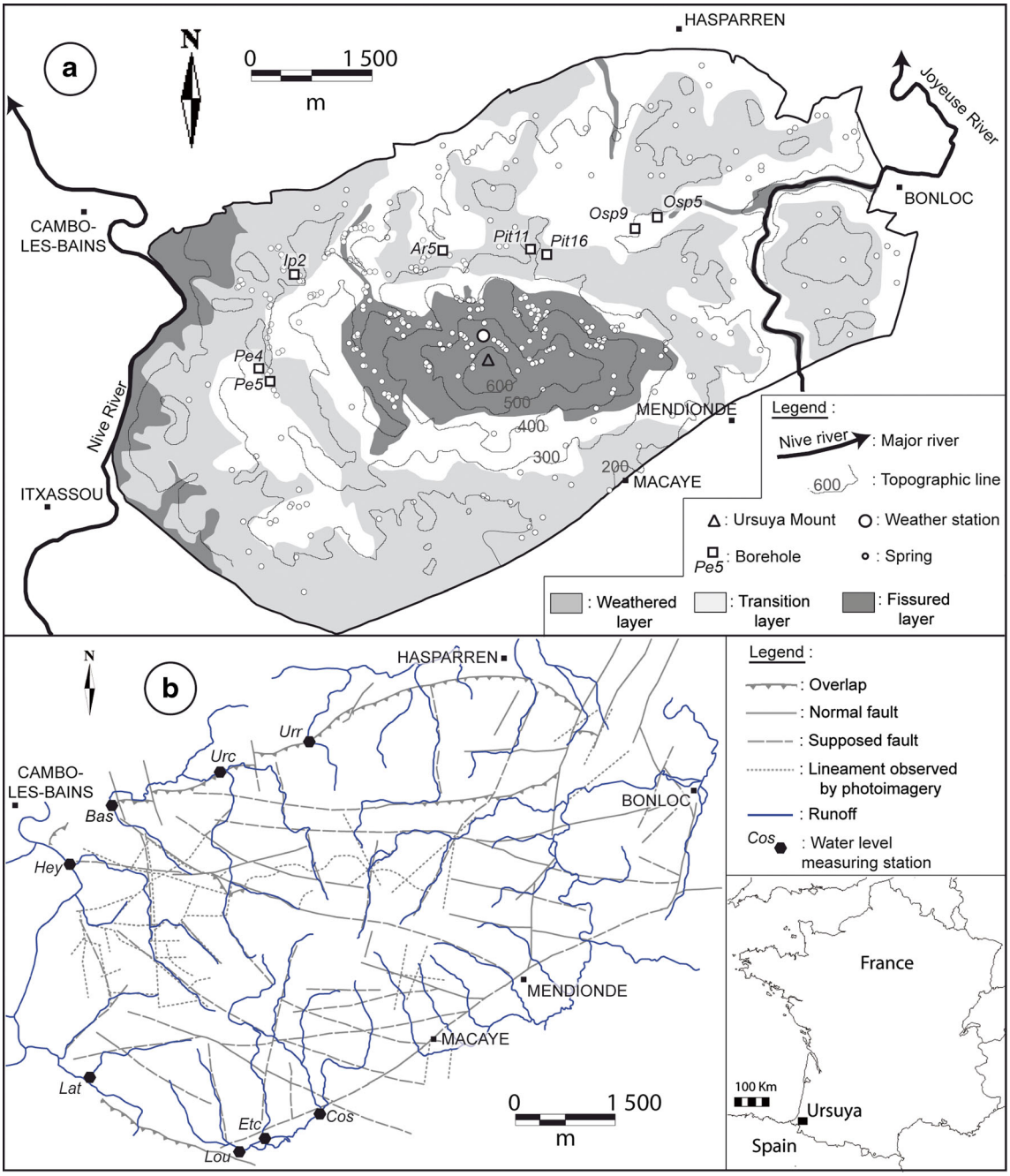

Fig. 1 **a** Ursuya Massif topography, lithology and location of monitoring points; **b** discontinuities runoff network and location of gauging stations. These maps are the result of the combination of Boissonnas et al. (1974) data, aerial photo imagery interpretation, field observations and drill cutting information

Hydroclimatology

Recorded data

The climate of the study area is temperate oceanic. The mean annual precipitation amount in the weather station of Biarritz-Anglet, 25 km from the study area (−1°31′54″; 43°28′18″; 69 mASL), is about 1,510 mm y^{-1} (calculated from 1964–2012 data from Meteo France). The estimated effective rainfall, using a Penman–Monteith computation, is 653 mm y^{-1} (Jaunat et al. 2013). The effective rainfall is the amount of rainfall remaining after evapotranspiration and which will be available for both runoff and groundwater recharge (Hiscock 2005).

Rainfall height (mm), air temperature, relative humidity, wind speed, sunshine and atmospheric pressure have also been measured directly at a dedicated weather station on the Ursuya Massif (550 mASL, Fig. 1a) during the study period.

The knowledge of these parameters provides an accurate characterisation of annual precipitation but also evapotranspiration and effective rainfall of the study area. The mean annual precipitation and estimated effective rainfall on the Ursuya Mount, calculated from this monitoring during the 3 years of measurements, are 1,440 and 624 mm y^{-1} respectively. The effective rainfall corresponds to 43 % of the total precipitation, which is similar to the Meteo France record at the weather station of Biarritz-Anglet (43 % for 1964–2012).

Climate projections

Besides high uncertainties, Pagé and Terray (2010) and Chauveau et al. (2013) agree with a decreasing trend of precipitation in the southwest of France (from 0 to −15 % until 2070) especially in western Pyrenees. For temperature, an increase between 1.5 and 2.8 °C is expected until 2050 for the southwest of France, but the Atlantic Ocean has a high capacity to absorb energy and to reduce the warming rates in the areas near the coast (Merot et al. 2013). The rising temperatures will result in an increase in the evapotranspiration rate and consequently, combined with a decrease in rainfall amount, aquifer recharge is expected to decrease in the Western Pyrenees region for the next few decades.

Hydrogeological properties

Significant groundwater flows take place in these formations. Between 1994 and 2003, 43 boreholes were drilled over the Ursuya Massif area in order to respond to the increasing water demand in the north-western Pyrenees. Of these boreholes, 34 were dry or too unproductive to allow viable sustainable exploitation. Presently, only 8 boreholes still exist on the study area (Fig. 1a and Table 1), of which merely 5 are operating (Osp5, Ar3, Ar5, Pit11 and Pit16). These boreholes have allowed lots of geological observations despite the few hydrodynamic investigations that were carried out. The hydraulic conductivities vary from $2 \cdot 10^{-7}$ to $1 \cdot 10^{-4}$ m s^{-1}, storage coefficients from $9 \cdot 10^{-5}$ to $1 \cdot 10^{-2}$ and transmissivity from $1 \cdot 10^{-5}$ to $4 \cdot 10^{-3}$ m s^{-2}. These values and the observed heterogeneity are characteristic of fissured media (Blouin et al. 2013; Dewandel et al. 2005; Maréchal et al. 2004; Taylor and Howard 2000). In addition to these boreholes, 190 springs have been recognized among which 101 are exploited (Fig. 1a). These springs feed an important surface flow network often developed along discontinuities (Fig. 1b). This surface drainage system is in constant relation with groundwater, draining or feeding it, depending on the geological and geomorphological contexts and also on the hydrodynamic level of the water table.

Based on groundwater geochemistry, isotopic analyses, modelled ages and the lithological conditions described earlier, different flowpath configurations have been described for the aquifer of the Ursuya Massif in Jaunat et al. (2012). Thus, in the fissured zone, when it is outcropping, the shallow water flows rapidly along the fissures of the gneissic rock. Where the fissured layer is underlying a weathered one, the groundwater can circulate in both. According to the degree of weathering, mixing between water from these two layers is allowed.

Methods

Groundwater modeling

The numerical translation of the conceptual model described previously has been realized in finite elements with the FEFLOW code 6.0 (Finite Element Subsurface Flow and Transport Simulation System; Trefry and Muffels 2007). The development of a numerical hydrodynamic model requires several steps: implementation of geometry, hydrodynamic parameters, values of recharge rates and volumes of groundwater withdrawals.

Table 1 Characteristics of the boreholes existing in the study area

BH name	Exploitation	Longitude (°/min/s)	Latitude (°/min/s)	*Z* (mASL)	Depth (m)	Layer exploited	*K* (m s^{-1})
Ar5	Exploited	−1 2021.2	43 2123.9	265	43	Fissured[a]	NM
Pit11	Exploited	−1 1937.7	43 2121.3	280	41	Fissured[a]	NM
Pit16	Exploited	−1 1947.2	43 2123.0	310	52	Fissured[a]	NM
Osp5	Exploited	−1 1836.2	43 2140.8	170	58	Fissured[a]	NM
Osp9	Non exp.	−1 1853.8	43 2136.2	175	55	Fissured[b]	$2.20 \cdot 10^{-7}$
Pe4	Non exp.	−1 223.3	43.2026.9	215	47	Trans. + Fissured[b]	$6.75 \cdot 10^{-5}$
Pe5	Non exp.	−1 2154.4	43 2025.2	215	42	Trans. + Fissured[b]	$1.10 \cdot 10^{-4}$
Ip2	Non exp.	−1 2158.2	43 2119.7	150	57	Fissured[b]	$6.70 \cdot 10^{-6}$

Trans. transition, *NM* not measured, *Z* elevation, *K* hydraulic conductivity

[a] Data from operators

[b] Data from borehole logging conducted during this study

Horizontal and vertical discretization

The extent of the numerical model covers an area of 45 km^2 discretized via a triangular mesh of 74,777 elements per layers (Fig. 2a). This irregular triangulation is based on the set of points with available information; thus, the mesh is refined around springs, wells, streams and along the mapped lineaments.

The vertical discretization of the different layers has been reproduced through five calculation layers: the weathered layer, the transition one, two fissured layers and the bedrock. Paragneisses and gneisses, with similar hydraulic characteristics, have not been distinguished in the numerical model.

The representation of the horizontal extension of these layers is based on the local map (Fig. 1a). The vertical extent of each layer was approached through the lithological descriptions obtained from the 26 drillings conducted on this area over the past decades and for which information is available, literature review—Table S1 of the electronic supplementary material (ESM) and field investigations.

The weathered layer, when existing, is represented by a layer, 20 m thick maximum with an increasing thickness gradient (Fig. 2b). The transition layer between weathered and fissured materials is simulated through a layer 10 m thick maximum also with a thickness gradient. The two fissured layers are simulated by an upper layer 15 m thick and a maximum thickness of the underlying layer of 20 m (Fig. 2b). The hard rock basement is simulated through an idealized layer hydrodynamically homogenous with negligible hydraulic conductivity and specific storage ($K = 1 \cdot 10^{-9}$ m s^{-1} and $S_s = 1 \cdot 10^{-6}$ m^{-1}; e.g. Maréchal et al. 2004; Walker et al. 2001) and highly thick (from the bottom of the fissured layer to −600 mASL) avoiding edge effects in the numerical calculations.

Input and calibration data

Boundary conditions

Potential groundwater flows and exchanges through the limits of the aquifer have been computed with fixed hydraulic heads (Dirichlet-type boundary conditions). Only the western limit formed by the Nive River (Fig. 1) is simulated through Cauchy-type boundary conditions. The relationships between the surface flow network and the sub-surface were also simulated by Cauchy-type boundary conditions all over the modelled area. These boundary conditions allow simulation of interactions between streams and groundwater, through a layer that is more or less clogged (Diersch 2010; Trefry and Muffels 2007). The transfer rate is then defined through this conductance parameter which has been adjusted during the calibration procedure.

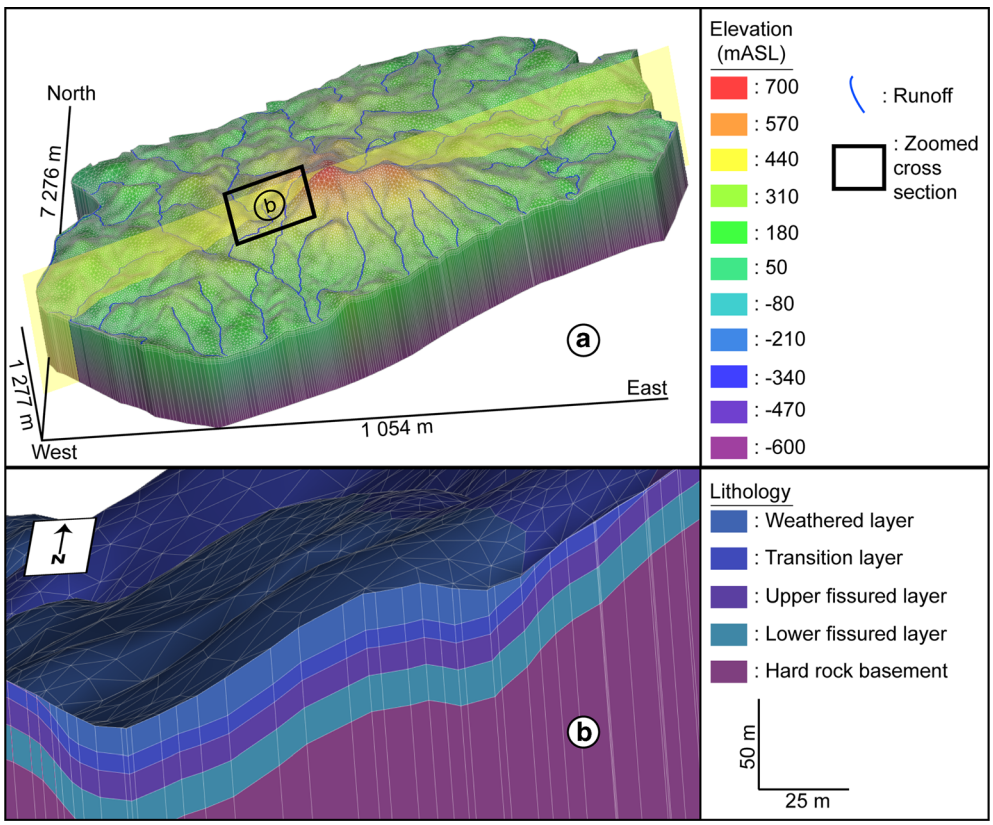

Fig. 2 Geometry of the finite element groundwater model (a magnification factor of 2 is applied to the vertical axis; **a** full area; **b** zoomed cross section)

Hydrodynamic parameters

In order to simulate accurate groundwater flow, the values of specific storage and hydraulic conductivity used in the model are based on data from pumping tests conducted in the non-exploited boreholes still existing on the study area (Table 1). Given the low density of this dataset and its poor spatial distribution, a bibliographical review has been conducted in order to ascertain and validate hydrodynamic parameters of the different layers of the weathered profile of the aquifer of the Ursuya Massif (Table S2 of the ESM). These values were then adjusted during the calibration phase in steady state and transient regimes. These adjustments are based on lithological and structural properties and concern especially major fractures that can act as preferential flow pathway. Data on aperture, filling, continuity or wall roughness for individual discontinuities are inaccessible at the study site scale. Nevertheless, the localization of the discontinuities network (Fig. 1b) has been essential in the calibration process in order to implement preferential flow conditions along it and to ascertain its role in the groundwater flows. Lithological field observations were also relevant to adjust hydrodynamic properties. Thus, clay and sand contents in weathered and transition layers, presence of pegmatite and metamorphosed limestone lenses, and rate of fissuring of the fissured layers are some properties that were used to localize adjustments of hydrodynamic parameters in a realistic way.

Recharge, withdrawals and hydraulic head

The weekly volumes of withdrawals in the exploited boreholes (Ar5, Osp5, Pit11 and Pit 16; Fig. 1a) were provided by operators. The measured hydraulic heads (hourly to weekly time steps based on different operators) have been used for the model calibration at transient state.

Hydraulic heads of non-exploited boreholes (Ip2, Osp9, Pe4 and Pe5; Fig. 1a) and runoff volumes recorded at the height gauging stations (Fig. 1b) have also been used for the model calibration. Hydraulic heads in non-exploited boreholes and water levels in streams were measured by automatic water level sensors "Schlumberger Mini-Diver" and were recorded at an hourly time step. For the streams, five to seven gaugings per station were conducted, distributed throughout the water cycle, in order to convert the measured water level to flow rate. These measurements were conducted continually between August 2009 and June 2012.

The monitoring of weather parameters directly at the study site allows one to define accurate precipitation conditions and effective rainfall amount on a weekly basis. The recharge of the aquifer (part of the effective rainfall that reaches the saturated zone) has been computed based on these results, and considering the influences of the vegetation cover and the soil characteristics on the amount of infiltrated water. Then, different sectors where defined from this analyse and adjusted during the steady-state calibration phase, with extreme amounts of infiltration water between 20 % of the effective rainfall (mean about 80.4 mm y^{-1}) where the soil is thick and strongly clayey and 90 % of the effective rainfall (mean about 400 mm y^{-1}) where the soil is absent as is the vegetal cover (Armand et al. 1995). The mean annual volume of recharge water computed using these values corresponds to $8.3 \cdot 10^6$ m^3 y^{-1} for the whole study area, which represents 0.2 m^3 m^{-2} y^{-1}.

Predictive simulation and groundwater response to climate change

Data used

In this study, spatial data from SCRATCH2010 models (produced by the CERFACS; European Centre for Research and Advanced Training in Scientific Computation; Pagé and Terray 2010), updated in 2012, has been used. The spatial resolution is about 8 km, with a monthly time step. The method of downscaling used for the production of these data is widely developed in Boé et al. (2006) and Boé and Terray (2008). This treatment was performed on data from the ARPEGE models V4.6 (research action on small and large scale) produced by the CNRM (National Centre for Meteorological Research).

Precipitation data and effective precipitation resulting from the A2 and B1 scenarios have been used in this study. The A2 and B1 scenarios, which were developed by the Intergovernmental Panel on Climate Change (IPCC), reflect two contrasting future greenhouse gas emission situations based on different hypotheses of economy and population trends in the future (IPCC 2013, 2014; Nakicénovic et al. 2000). A2 is characterized by high emissions of greenhouse gases and is considered as a pessimistic scenario, while B1 is considered as an optimistic one.

Simulation of climate change scenarios

Forecast simulations were performed for a period of 49 years, between 2001 and 2050. A monthly time step was adopted for these simulations and the amount of recharge water was estimated using the data presented earlier from the predictive scenarios. The forecasted amounts of effective precipitation have then been corrected with the soil and the vegetation factors previously discussed, in order to consider only the infiltration water in the numerical model.

The groundwater withdrawals were also introduced to achieve these forward simulations. Average monthly volumes were calculated using the 3 years of available data (July 2009 to July 2012). These monthly withdrawals were repeated identically during the 49 years of simulation. Without precise predictive demographic data, this treatment seems appropriate for

the evaluation of the impact of climatic trends on groundwater resources in a realistic way (this fact will be discussed later on).

Results and discussion

Calibration and validation of the numerical model

Steady-state calibration

The numerical model has been initially calibrated in steady state, using the 2011 data, a period for which the available dataset is the most complete. This step allowed a first assessment of the model characteristics before switching to the transient state regime.

The steady-state calibration was based on the altitude of the 198 perennial springs identified in the study area. The steady-state calibration consisted of the restitution by the model of a hydraulic head pattern in agreement with the seeping altitude of these springs (Fig. 3). At the end of the calibration phase, 170 observation points showed a difference of less than 10 m between simulated and observed hydraulic heads, of which 120 are less than 5 m. Differences of about 10–15 m were observed for 22 calibration points and the simulated levels presented a difference of 15–20 m with the measured altitude for six springs. Besides this good correlation between computed and observed hydraulic heads, the mean absolute error (MAE, corresponding to the mean of the absolute value of the residual, Anderson et al. 2015) about 0.89 m revealed an overall good result.

The 3-year runoff-volume dataset has also been used for the calibration procedures. The exploited volumes from the springs emerging in the eight controlled watershed (Urr, Urc, Bas, Hey, Lat, Lou, Etc., Cos, Fig. 1b) were added to that measured at the gauging stations, in order to precisely identify groundwater outflows in these areas. These volumes were compared with the simulated outflows from the numerical model for the same areas. The results showed a positive correlation between simulated and measured outflows.

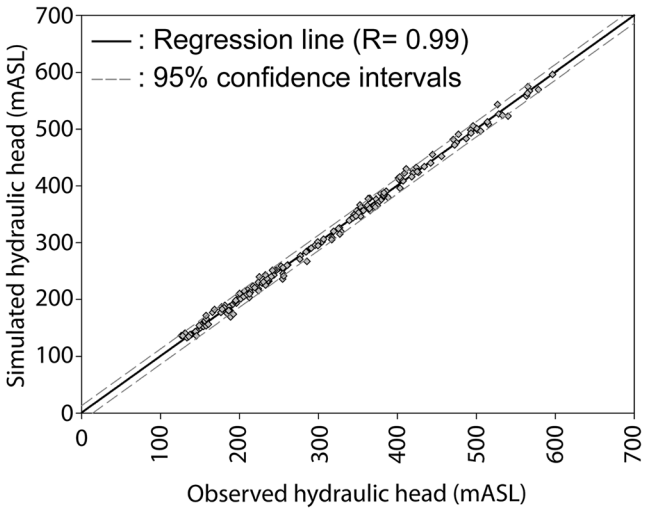

Fig. 3 Correlation between simulated and observed hydraulic heads in steady state

The simulated outflow for the whole watershed was slightly higher than the measured one (respectively 11,682,693 and 11,149,625 m^3 y^{-1}), with a ratio [simulated volumes/measured volumes] of about 0.95.

Transient calibration

In a transient regime calibration, the simulation period should be long enough and the data available have to be adequate, accurate and complete. On the Ursuya Massif, recharge data, withdrawals and hydraulic head variations have been precisely recorded since July 2009. These data are recorded in different time steps (from hourly for recharge and hydraulic heads to weekly for exploited volumes); therefore, the model is calibrated in transient state over a period of 3 years (July 2009 to July 2012), at a weekly time step. Hourly values of recharge have been summed on a weekly basis and weekly means of hydraulic heads have been used for the calibration. Results are presented at an annual scale so as to facilitate the reporting of results.

The comparison of measured and simulated hydraulic heads shows a good restitution of the water table by the model (Fig. 4). The total mean absolute error (MAE) of about 1.9 m confirms the realism of the numerical model. The individual MAE is less than 1 m for the boreholes Ar5, Osp9 and Ip2 (respectively 0.74, 0.29 and 0.32 m, Fig. 4). It is slightly higher for Pit11, Pe5, Pe4 and Osp5 (respectively 1.56, 1.38, 2.62, 6.44 m, Fig. 4) but in an acceptable range beside the range of hydraulic heads variability of these boreholes.

Accuracy of flow conditions through hydrodynamic numerical modeling

The hydrodynamic properties of the calculation layers used in the numerical model of the Ursuya aquifer are presented in Fig. 5. Values of hydraulic conductivity are computed based on the local dataset and bibliographical review and are adjusted through the calibration process in steady and transient regimes. These implemented hydrodynamic properties allow for representing flow conditions quite close to field observations, and describe the strong influence of the weathered profile and of the hard rock discontinuities on the groundwater flow in crystalline aquifers.

These results allow the establishment of a conceptual model available for weathered hard rock aquifers with

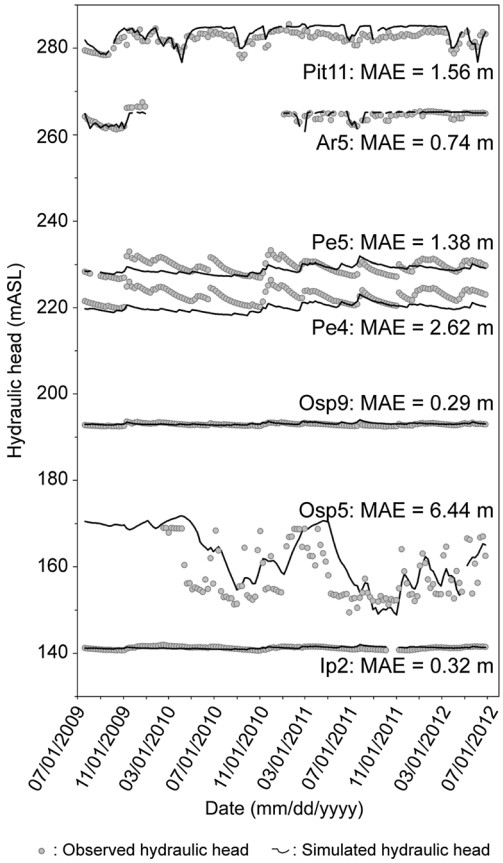

Fig. 4 Simulated and observed hydraulic heads in transient state for boreholes between July 2009 and July 2012. *MAE* mean absolute error

heterogeneous geographical weathering and erosion mechanisms (Fig. 5; Table 2):

1. The weathered layer, besides having a high porosity, always has low permeability ($5 \cdot 10^{-8} \leq K \leq 5 \cdot 10^{-7}$ m s^{-1} in the Ursuya Massif). This layer, when saturated, is considered as a capacitive one and ensures a storage function. The lowest values are here linked to differential weathering processes due to the presence of pegmatite (Boissonnas et al. 1974; Ondarroa et al. 1998) in one area of the study site (Olhasso on Fig. 5).
2. In the transition layer, the original structure of the bedrock is preserved. It is thus possible to observe the influence of regional fractures in this layer with higher values along major discontinuities ($1 \cdot 10^{-6} \leq K \leq 1 \cdot 10^{-5}$ m s^{-1}). However, beside these preferential pathways, this layer displays a quite low permeability ($7 \cdot 10^{-8} \leq K \leq 3 \cdot 10^{-7}$ m s^{-1}).
3. The fissured layer is generally characterized by a dense fissuring network and ensures a transmissive function along active discontinuities ($1 \cdot 10^{-6} \leq K \leq 5 \cdot 10^{-4}$ m s^{-1}). In addition, this study's results highlight the fact that the erosion process has to be considered. Indeed, where the weathered profile is complete, the hydraulic conductivity of the lower fissured layer is higher than that of the upper one ($1 \cdot 10^{-6}$ and $8 \cdot 10^{-7}$ m s^{-1} respectively).
4. Where the transitional and/or weathered materials are eroded, and in case of regional extent erosion processes, the porosity of the fissured layer could be clogged ($4 \cdot 10^{-8}$–$7 \cdot 10^{-8}$ m s^{-1} for the upper fissured layer and $4 \cdot 10^{-8}$–$3.5 \cdot 10^{-8}$ m s^{-1} for the lower fissured one in Petchoenea zone and Ursuya Mount area in Fig. 5), except along some of the major discontinuities. A multiple phasing of the weathering processes can then be suspected. Fissures are progressively filled up by clay-rich materials and are then obliterated by the weathering process (Dewandel et al. 2006). These sealed fissures explain the low permeability observed in these parts of the aquifer.
5. On the other hand, if the weathered material's disappearance is the result of recent fluvial erosion, it could be expected that the local porosity of fissures is still conductive and that the global hydraulic conductivity of the fissured layer is favourable to groundwater flow. This can be observed along the Nive River (Fig. 5), where the lack of weathered and transitional materials is related to mechanical processes, induced by fluvial erosion. In this case, the recent erosion of the unconsolidated surrounding materials allows a favourable porosity (Cho et al. 2003; Dewandel et al. 2006; Lachassagne et al. 2001; Taylor and Howard 2000) for both the upper and the lower fissured layers, with the value of K respectively between $7 \cdot 10^{-6}$ and $1 \cdot 10^{-6}$ m s^{-1}.

This model, displayed in Table 2, is in agreement with the results obtained during the past few decades on weathered profiles of crystalline aquifers (Acworth 1987; Courtois et al. 2010; Dewandel et al. 2006, 2011; Houston and Lewis 1988; Howard et al. 1992; Lachassagne et al. 2011; Maréchal et al. 2004; White et al. 2001; Wyns et al. 2004).

In the Sohano and Mendurria zones, the permeability is also lower, with values respectively between $4 \cdot 10^{-8}$ and $8 \cdot 10^{-7}$ m s^{-1} for the upper fissured layer and $3.5 \cdot 10^{-8}$ and $1 \cdot 10^{-7}$ m s^{-1} for the lower one. Unfortunately, these geographical sectors have never been subject to drilling and no data exist. The lack of knowledge around these areas does not allow for conclusions on the origin of the low permeability values; however, even if uncertainties remain about the geometry and the hydrodynamic properties implemented in these zones, they allow a realistic transcription of the global morphology of the hydraulic heads.

In the same way as for hydraulic conductivities, data on specific storage are based on local datasets and bibliographical review. They were then adjusted through the calibration process in a transient state regime. For the weathered layer, values from $1.3 \cdot 10^{-4}$ to $5.5 \cdot 10^{-3}$ m^{-1} are reported in the literature

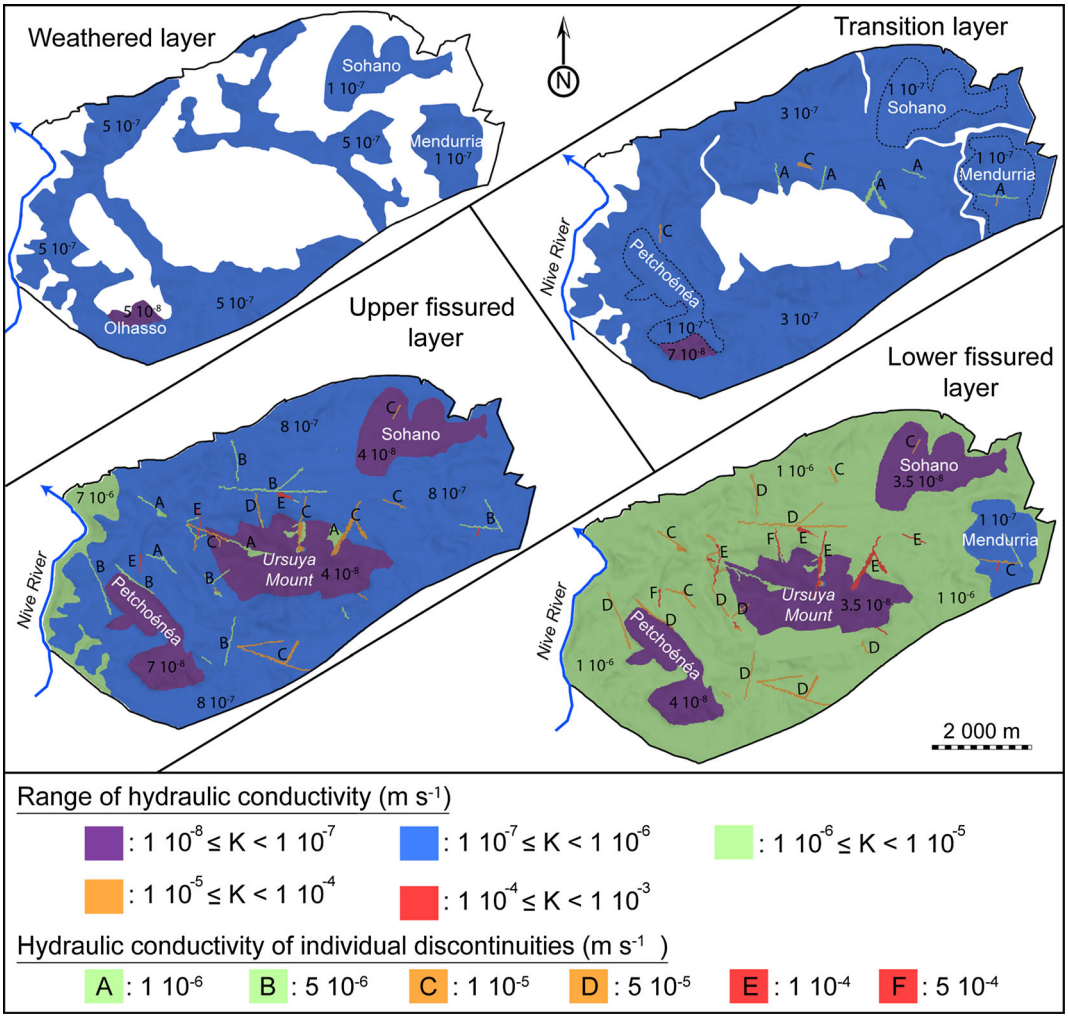

Fig. 5 Maps of computed hydraulic conductivity for the four first layers. (Not shown: hydraulic conductivity of bedrock horizon is homogeneous with a value about $1 \cdot 10^{-9}$ m s^{-1})

(Dewandel et al. 2006; Domenico and Mifflin 1965), whereas concerning the fissured layer, values between $3.3 \cdot 10^{-6}$ and $7.0 \cdot 10^{-3}$ m^{-1} are proposed (Dewandel et al. 2011; Domenico and Mifflin 1965; Lee and Lee 2000). The values obtained for the aquifer of Ursuya after the calibration phase are about $5 \cdot 10^{-4}$ m^{-1} for the weathered layer, $1 \cdot 10^{-4}$ m^{-1} for the transition layer, and $5 \cdot 10^{-5}$ m^{-1} for the two fissured layers. For these two layers, S_s is locally higher along some discontinuities ($1 \cdot 10^{-4}$–$5 \cdot 10^{-4}$ m^{-1}).

Impact of climate change on water resources

Recharge evolution

Future rainfall amount and effective precipitation estimated until 2050 are presented, at an annual time step, in Fig. 6. According to the A2 scenario, in the study area, annual rainfall amount is decreasing between 2001 and 2050 (−5.0 mm y^{-1}; $R = 0.4$) as is effective precipitation (−5.6 mm

Table 2 Ranges of hydraulic conductivities K (m s^{-1}) imputed in the Ursuya aquifer numerical model and summary of K along the weathered profile

Layer		K, profile complete	K, transitional and/or weathered layer absent	
Weathered	–	$5 \cdot 10^{-8} \le K \le 5 \cdot 10^{-7}$	Regional erosion processes	Recent fluviatile erosion
Transition	Global	$7 \cdot 10^{-8} \le K \le 3 \cdot 10^{-7}$		
	Discontinuities	$1 \cdot 10^{-6} \le K \le 1 \cdot 10^{-5}$		
Upper fissured	Global	$8 \cdot 10^{-7}$	$4 \cdot 10^{-8} \le K \le 7 \cdot 10^{-8}$	$7 \cdot 10^{-6}$
	Discontinuities	$1 \cdot 10^{-6} \le K \le 5 \cdot 10^{-4}$	$1 \cdot 10^{-6} \le K \le 5 \cdot 10^{-4}$	$1 \cdot 10^{-6} \le K \le 5 \cdot 10^{-4}$
Lower fissured	Global	$1 \cdot 10^{-6}$	$3.5 \cdot 10^{-8} \le K \le 4 \cdot 10^{-8}$	$1 \cdot 10^{-6}$
	Discontinuities	$1 \cdot 10^{-5} \le K \le 5 \cdot 10^{-4}$	$5 \cdot 10^{-6} \le K \le 5 \cdot 10^{-4}$	$5 \cdot 10^{-6} \le K \le 5 \cdot 10^{-4}$

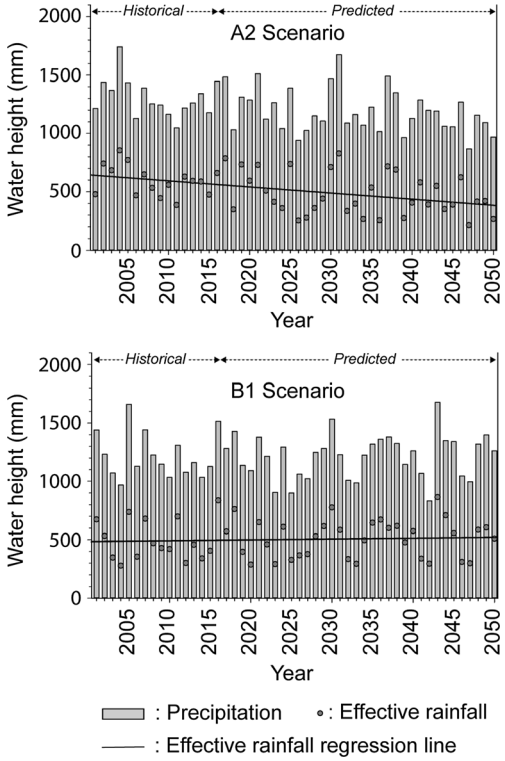

Fig. 6 Forecast of annual rainfall and effective precipitation (with corresponding regression lines: $a_{A2} = -5.6$ mm y^{-1} and $R_{A2} = 0.42$; $a_{B1} = 0.3$ mm y^{-1} and $R_{B1} = 0.02$) in the north-western Pyrenees until 2050, according to scenarios A2 and B1

y^{-1}; $R = 0.4$). Indeed, despite low correlation coefficients induced by significant inter annual variations, a decreasing trend is highlighted (Fig. 6). The average rainfall calculated from data according to the B1 scenario between 2001 and 2050 does not show any declining trend, and neither does the effective precipitation (Fig. 6). According to the B1 scenario, the hydroclimatology of the region should be exposed to only little changes, thus this climatological hypothesis has not been simulated.

Impact of climate change on hydraulic heads and groundwater storage

Estimated changes in rainfall amount are relatively low until 2050 in the north-western Pyrenees (Fig. 6), similarly the changes in groundwater heads and aquifer storage. The computation of the annual hydraulic head median is presented in Fig. 7, according to the forecasted scenario A2, for the eight monitored boreholes.

These simulated hydraulic heads show heterogeneous decreasing trends with a maximum depletion of -0.13 m y^{-1} for Pit16 (decrease in head about 5.85 m over 45 years) and a minimum of $-2.6\ 10^{-3}$ m y^{-1} for Ar5 (decrease in head about 0.12 m over 45 years). The significance of this decreasing trend is not robust regarding the linear correlation coefficient for Ar5 and Osp9 (correlation coefficient of 0.30 and 0.40 respectively; Fig. 7). For the other observation points, the correlation is higher: R values from 0.49 (Pit16) to 0.73 for Pe4. The global mean of decrease in heads is about −2.12 m between 2005 and 2050 and is in the range of inter-annual variations of hydraulic heads.

Hydraulic heads observed from the few boreholes existing on the Ursuya Massif offer only a local vision of the hydrodynamic evolution of the aquifer. Groundwater storage is more representative at the aquifer scale. Figure 8 represents the annual volumes outgoing and ingoing the system and the annual balance. The outgoing volumes include natural and artificial ones, with an average groundwater storage withdrawal from boreholes of about 5,000 m^3 y^{-1}. A logical correlation appears clearly between the storage fluxes computed and recharge amount estimations (Fig. 6). Thus, groundwater storage is in deficit during the driest years (e.g. 2006 in the historical period, 2018 and 2026 in the projected period), while the balance is positive during the rainy years (e.g. 2004 in the historical period, 2025 and 2030 in the projected period); however, the simulations do not highlight a reliable long-term trend, and consequently do not highlight a long-term trend for the recharge evolution in the coming decades.

The low impact of changes in recharge is thus clearly highlighted by the evolution of groundwater storage. These results also show that groundwater depletion by actual borehole exploitation is negligible beside the groundwater storage variations generated by inter-annual variations in recharge amount.

Impact of climate change on natural discharges

In order to precisely determine the potential changes on a global scale, the natural aquifer discharges have been computed to assess the groundwater volume variations in response to climate change. Therefore, this computed discharge represents the outflows of springs, which are used for drinking water and/or generate runoff on the Ursuya Massif (Fig. 1b); furthermore, the methodology used for the calibration procedure shows that the natural groundwater outflow is well transcribed by the numerical model.

The simulated annual median of natural discharge (Fig. 9) shows a significant decreasing trend of -360 m^3 y^{-1} ($R = 0.6$) between 2001 and 2050. Assuming a linear decrease, without considering the inter-annual variations, this tendency would lead to a total decrease of about 17,640 m^3 of the natural outflow of the Ursuya aquifer in 2050, relative to the current discharge. Nevertheless, these results should be considered in the context of the actual exploited volumes from this aquifer ($1.5\ 10^6$ m^3 y^{-1} from the springs and $1.8\ 10^6$ m^3 y^{-1} with boreholes). The calculated 50-year decrease corresponds to only 1.3 % of the exploited volumes of spring water and to 1.1 % of the total collected volume.

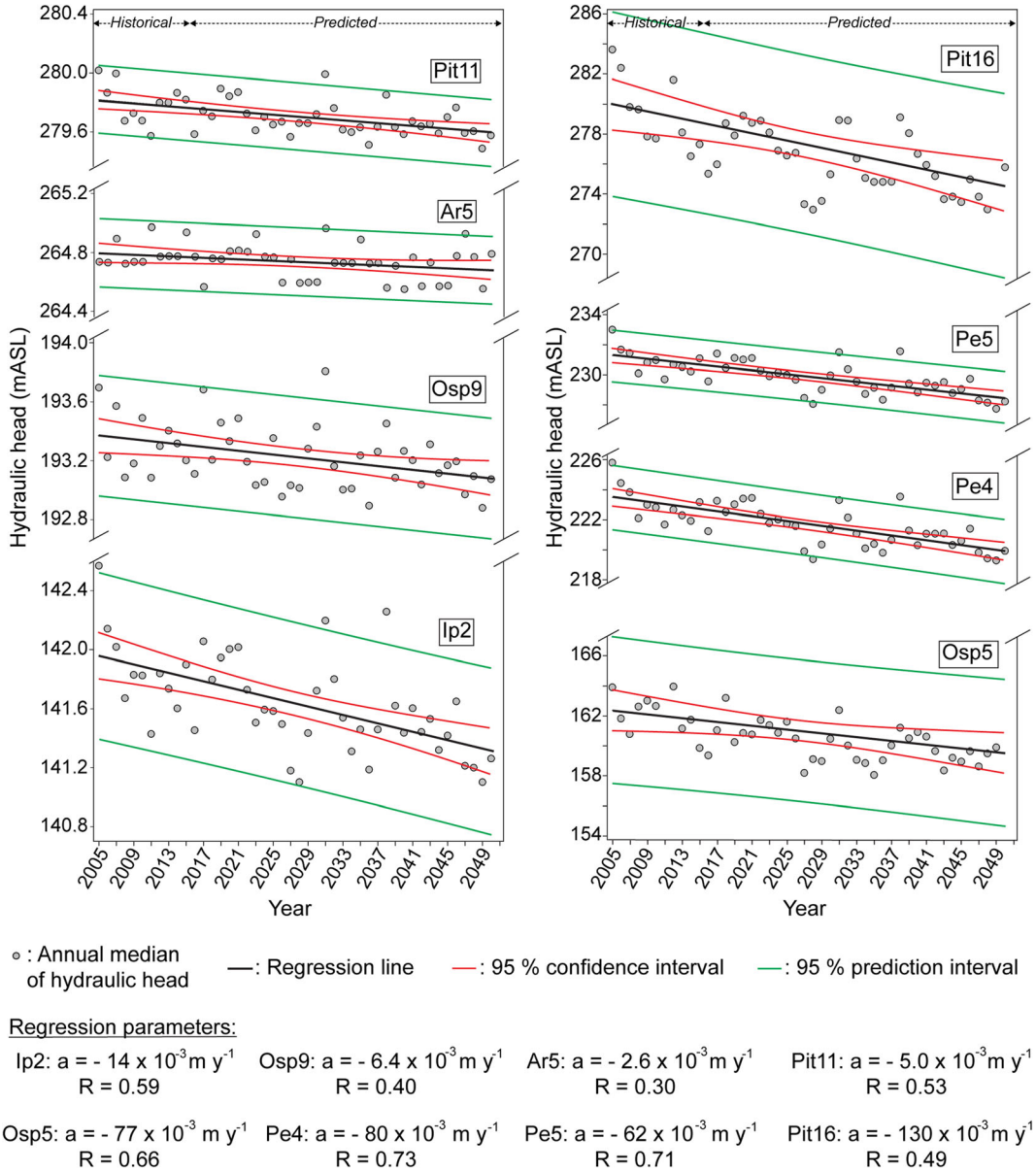

Fig. 7 Annual median of hydraulic heads in monitored boreholes simulated between 2005 and 2050 and corresponding regression line with 95 % confidence and prediction intervals

In conclusion, this long-term simulation, and the low decrease discharge calculated, has to be carefully considered. If climate change does not seem to be a crucial parameter in the five future decades for the Ursuya aquifer, longer simulations could show more worrying results.

Uncertainties and perspectives

The results of the simulation of climate change impacts on groundwater resources are naturally affected by a number of uncertainties (Demissie et al. 2015). Among them, some inaccuracies in the input geometry and hydrological data are difficult to avoid in numerical groundwater models at the aquifer scale (Ghanbari and Bravo 2011; Refsgaard et al. 2010), mainly because of the poor distribution of field data. Another source of inaccuracies in forecast models lies in the input of hydroclimatic data, the predictions of the future climatic variables (Nakicénovic et al. 2000) and the limitations of the current downscaling techniques (Jackson et al. 2011; Prudhomme and Davies 2008; Serrat-Capdevila et al. 2007). Therefore, it is obvious that the predictive modeling of groundwater evolution, under changing climate conditions, leads to an accumulation of uncertainties; thereby, the results of such simulations should be regarded only as a probable trend of evolution.

This tendency could largely be influenced by socio-economic development. On the one hand, the climate change models are based on worldwide socio-economic forecasts

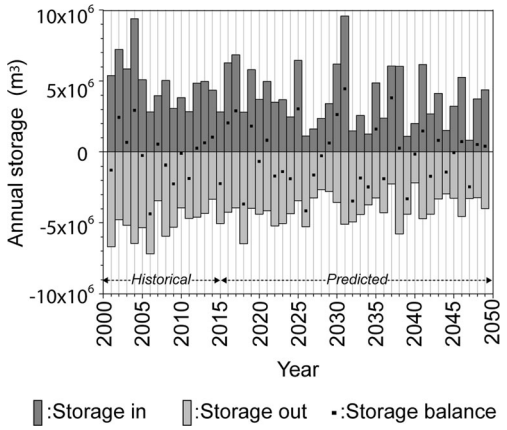

Fig. 8 Annual volumes outgoing and ingoing the system and annual balance

(Nakicénovic et al. 2000), while on the other hand, the local choices of policymakers have a strong influence on the groundwater evolution. Peculiarly, land cover changes will impact both the soil permeability and therefore the infiltration rate, as well as the groundwater use for irrigation purposes or alternatively for the drinking-water supply. Indeed, the evolution of groundwater use is another socio-economic parameter that should be considered regarding the demographic evolution. For example, in the Pyrénées-Atlantiques, which is the French administrative division where this study has been conducted, the forecasted demographic annual trend is between +7 and +12 % between 2010 and 2030 (INSEE 2010). It is then likely that the increase in water abstraction from the aquifer of Ursuya will be at least as impactful as the influence of climate change. Unfortunately, accurate prospective data on demographic and future water needs at a longer time scale, and at a local scale, are scarce, especially for such rural areas. In accordance with Döll (2009), Holman (2006), Holman et al. (2012), Kurylyk and MacQuarrie (2013), and Vouillamoz et al.

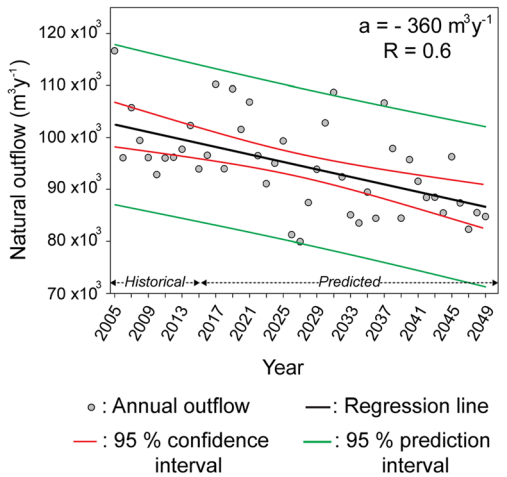

Fig. 9 Natural annual outflows simulated between 2005 and 2050 and corresponding regression line with 95 % confidence and prediction intervals

(2015), it seems unreasonable to project climate change for a century and assume that water supply needs and land cover conditions will be intransient. Half a century in scale seems to be the upper limit that groundwater modeling simulation can provide relevant information for, even regardless of future demographic and land use changes. Beyond that time, pertinent groundwater modeling simulation needs increased effort to assess future changes of the socioeconomic environment, land cover, water uses and climate conditions.

Summary and conclusions

In this study, a groundwater model of a singular fissured aquifer with a high degree of weathering has been developed. The proposed methodology combined the finite element numerical solution with the equivalent porous media model, to adequately model the hydrogeological characteristics measured on the crystalline aquifer of Ursuya. The geometry of the conceptual model of hard rock aquifers developed over the last decade (Wyns et al. 2004) has been numerically transcribed thanks to five calculated layers representing the weathering profile of such media—one weathered layer separated from the two fissured ones by a transition zone, overlying the hard rock basement. The monitoring network, deployed in 2009 on the study site, not only allowed the research team to obtain accurate data (meteorological data, hydrodynamic parameters, geometry of the system) that can be used in the numerical model, but it also confirms the very good agreement between simulated and measured parameters (notably for hydraulic heads and runoff volumes). Hydrodynamic properties of Ursuya aquifer were precisely described and the predominant influence of the weathered profile was clarified as well as the role of the geological discontinuities in such a hard-rock aquifer with a high degree of weathering.

Regarding the aim of long-term management of this resource, forecast simulations have been conducted based on the computed model. The most pessimistic climate projection (scenario A2 from the IPCC), at a half-century scale, in the north-western Pyrenees, shows a slight decreasing of the effective precipitation, around 5 mm y^{-1}. Groundwater modeling simulation from these data showed that climate change will not significantly modify the groundwater flows in the coming decades; nevertheless, a decrease in the flow of springs and streams is probable, but will not endanger the water resource. Longer simulations could show more worrying results, but it seems unreasonable to project climate-change-effect consequences beyond a 50-year forecast without precise socio-economic predictions on demographic trends, land use modifications and water-use evolution.

Acknowledgements This study has been financially supported by the "Conseil Régional d'Aquitaine", the "Agence de l'Eau Adour-Garonne" and "Conseil Général des Pyrénées Atlantiques" through the European

Regional Development Fund (ERDF) program. The authors would like to thank the municipalities of Bayonne, Hasparren and Cambo-les-Bains, and the SIAEPs of Mendionde-Bonloc and Macaye-Louhossoa for their support and contribution to the implementation of the project. The authors would also like to thank two anonymous reviewers for their valuable comments which helped to improve the quality of the manuscript.

References

Abusaada M, Sauter M (2013) Studying the flow dynamics of a karst aquifer system with an equivalent porous medium model. Ground Water 51:641–650

Acworth R (1987) The development of crystalline basement aquifers in a tropical environment. Q J Eng Geol 20:265–272

Aguilera H, Murillo J (2009) The effect of possible climate change on natural groundwater recharge based on a simple model: a study of four karstic aquifers in SE Spain. Environ Geol 57:963–974

Allen DM, Whitfield PH, Werner A (2010) Groundwater level responses in temperate mountainous terrain: regime classification, and linkages to climate and streamflow. Hydrol Process 24:3392–3412

Anderson MP, Woessner WW, Hunt RJ (2015) Applied groundwater modeling, 2nd edn. Academic, San Diego, 329 pp

Armand C, Saint-Marc E, Ligouret P (1995) Ursuya (64): partie est, carte de vulnérabilité des eaux souterraines et prospection géophysique [Ursuya (64): eastern part, groundwater vulnerability map and geophysical survey]. BRGM report no. N1917BOR4S95, BRGM, Orleans, France, 31 pp

Ayraud V, Aquilina L, Labasque T, Pauwels H, Molenat J, Pierson-Wickmann A, Durand V, Bour O, Tarits C, Le Corre P, Fourre E, Merot P, Davy P (2008) Compartmentalization of physical and chemical properties in hard-rock aquifers deduced from chemical and groundwater age analyses. Appl Geochem 23:2686–2707

Banks E, Simmons C, Love A, Caranswick R, Werner A, Bestland E, Wood M, Wilson T (2009) Fractured bedrock and saprolite hydrogeologic controls on groundwater/surface-water interaction: a conceptual model (Australia). Hydrogeol J 17:1969–1989

Berkowitz B (2002) Characterizing flow and transport in fractured geological media: a review. Adv Water Resour 25:861–884

Bertrand G, Celle-Jeanton H, Huneau F, Loock S, Renac C (2010) Identification of different groundwater flowpaths within volcanic aquifers using natural tracers for the evaluation of the influence of lava flows morphology (Argnat basin, Chaîne des Puys, France). J Hydrol 391:223–234

Bertrand G, Siergieiev D, Ala-Aho P, Rossi P (2014) Environmental tracers and indicators bringing together groundwater, surface water and groundwater-dependent ecosystems: importance of scale in choosing relevant tools. Environ Earth Sci 72:813–827

Bloomfield JP, Gaus I, Wade SD (2003) A method for investigating the potential impacts of climate-change scenarios on annual minimum groundwater levels. Water Environ J 17:86–91

Blouin M, Martel R, Gloaguen E (2013) Accounting for aquifer heterogeneity from geological data to management tools. Ground Water 51:421–431

Boé J, Terray L (2008) Régimes de temps et désagrégation d'échelle [Weather regimes and downscaling]. La Houille Blanche 2:45–51

Boé J, Terray L, Habets F, Martin E (2006) A simple statistical-dynamical downscaling scheme based on weather types and conditional resampling. J Geophys Res 111, D23106

Boissonnas J, Le Pochat G, Thibault C, Bernatzk M (1974) Carte géologique d'Iholdy au 1/50 000 [Geological map of Iholdy]. BRGM no. 1027, BRGM, Orleans, France, 36 pp

Boronina A, Renard P, Balderer W, Christodoulides A (2003) Groundwater resources in the Kouris catchment (Cyprus): data analysis and numerical modelling. J Hydrol 271:130–149

Bouraoui F, Vachaud G, Li LZX, Le Treut H, Chen T (1999) Evaluation of the impact of climate changes on water storage and groundwater recharge at the watershed scale. Clim Dyn 15:153–161

Brouyère S, Carabin G, Dassargues A (2004) Climate change impacts on groundwater resources: modelled deficits in a chalky aquifer, Geer basin, Belgium. Hydrogeol J 12:123–134

Carrera J, Heredia S, Vomvoris S, Hufschmied P (1990) Modeling of flow with a small fractured monzonitic gneiss block. In: Hydrogeology of low permeability environments. IAH Selected Papers 02, Heise, Hanover, Germany, pp 115–167

Chauveau M, Chazot S, Perrin C, Bourgin P-Y, Sauquet E, Vidal J-P, Rouchy N, Martin E, David J, Norotte T, Maugis P, De Lacaze X (2013) Quels impacts des changements climatiques sur les eaux de surface en France à l'horizon 2070 ? [What will be the impacts of climate change on surface hydrology in France by 2070?]. La Houille Blanche 4:5–15

Chilton P, Foster S (1995) Hydrogeological characterisation and water-supply potential of basement aquifers in tropical Africa. Hydrogeol J 3:36–49

Chilton P, Smith-Carington A (1984) Characteristics of the weathered basement aquifer in Malawi in relation to rural water supplies. In: Challenges in African hydrology and water resources. Proceedings of the Harare symposium, IAHS 144, IAHS, Wallingford, UK, pp 57–72

Cho M, Ha K-M, Choi Y-S, Kee W-S, Lachassagne P, Wyns R (2003) Relationship between the permeability of hard-rock aquifers and their weathered cover based on geological and hydrogeological observation in South Korea. In: IAH Conference on "Groundwater in fractured rocks", Prague, 15–19 September 2003

Cook P (2003) A guide to regional groundwater flow in fractured rock aquifers. CSIRO, Dickson ACT, Australia, 115 pp

Courtois N, Lachassagne P, Wyns R, Blanchin R, Bougaîré F, Somé S, Tapsoba A (2010) Large-scale mapping of hard-rock aquifer properties applied to Burkina Faso. Ground Water 48:269–283

Davison CC (1985) URL drawdown experiment and comparison with models, TR 375. Atomic Energy of Canada, Pinawa, MB

Demissie Y, Valocchi A, Cai X, Brozovic N, Senay G, Gebremichael M (2015) Parameter estimation for groundwater models under uncertain irrigation data. Ground Water 53:614–625

Dewandel B, Lachassagne P, Boudier F, Al-Hattali S, Ladouche B, Pinault J, Al-Suleimani Z (2005) A conceptual hydrogeological model of ophiolite hard-rock aquifers in Oman based on a multiscale and a multidisciplinary approach. Hydrogeol J 13:708–726

Dewandel B, Lachassagne P, Wyns R, Marechal J, Krishnamurthy N (2006) A generalized 3-D geological and hydrogeological conceptual model of granite aquifers controlled by single or multiphase weathering. J Hydrol 330:260–284

Dewandel B, Lachassagne P, Zaidi FK, Chandra S (2011) A conceptual hydrodynamic model of a geological discontinuity in hard rock aquifers: example of a quartz reef in granitic terrain in South India. J Hydrol 405:474–487

Diersch HJG (2010) FEFLOW finite element subsurface flow and transport simulation system reference manual. DHI-WASY, Berlin, 292 pp

Djebebe-Ndjiguim CL, Huneau F, Denis A, Foto E, Moloto-A-Kenguemba G, Celle-Jeanton H, Garel E, Jaunat J, Mabingui J, Le Coustumer P (2013) Characterization of the aquifers of the Bangui urban area as an alternative drinking water supply resource. Hydrol Sci J 58:1760–1778

Döll P (2009) Vulnerability to the impact of climate change on renewable groundwater resources: a global-scale assessment. Environ Res Lett 4:035006

Domenico PA, Mifflin MD (1965) Water from low-permeability sediments and land subsidence. Water Resour Res 1:563–576

Eckhardt K, Ulbrich U (2003) Potential impacts of climate change on groundwater recharge and streamflow in a central European low mountain range. J Hydrol 284:244–252

Engeser T, Schwentke W (1986) Towards a new concept of the tectogenesis of the Pyrenees. Tectonophysics 129:233–242

Feuillée P, Rat P (1971) Structures et paléogéographie pyrénéo-cantabriques [Pyrenean-Cantabrian structures and paleogeography]. In: Histoire structurale du golfe de Gascogne [Structural history of the Bay of Biscay, vol 1]. Technip, Île-de-France, France, pp 1–48

Ghanbari RN, Bravo HR (2011) Coherence among climate signals, precipitation, and groundwater. Ground Water 49:476–490

Glynn P, Plummer L (2005) Geochemistry and the understanding of ground-water systems. Hydrogeol J 13:263–287

Hiscock K (2005) Hydrogeology: principles and practice. Blackwell, 389 pp

Holman I (2006) Climate change impacts on groundwater recharge: uncertainty, shortcomings, and the way forward? Hydrogeol J 14:637–647

Holman IP, Allen DM, Cuthbert MO, Goderniaux P (2012) Towards best practice for assessing the impacts of climate change on groundwater. Hydrogeol J 20:1–4

Houston J, Lewis R (1988) The Victoria Province Drought Relief Project, II: borehole yield relationships. Ground Water 26:418–426

Howard K, Hugghes M, Charlesworth D, Ngobi G (1992) Hydrogeologic evaluation of fracture permeability in crystalline basement aquifers of Uganda. Appl Hydrol 1:55–65

Hrkal Z, Milicky M, Tesar M (2009) Climate change in Central Europe and the sensitivity of the hard rock aquifer in the Bohemian Massif to decline of recharge: case study from the Bohemian Massif. Environ Earth Sci 59:703–713

Hsieh PA, Neuman SP (1985) Field determination of the three-dimensional hydraulic conductivity tensor of anisotropic media: 1. theory. Water Resour Res 21:1655–1666

INSEE, Department of Demography (2010) www.bdm.insee.fr. Accessed March 2016

IPCC (2013) Climate change 2013: the physical science basis. Contribution of Working Group I to the Fifth Assessment Report of the Intergovernmental Panel on Climate Change. Cambridge University Press, Cambridge, 1535 pp

IPCC (2014) Climate change 2014: synthesis report. Contribution of Working Groups I, II and III to the Fifth Assessment Report of the Intergovernmental Panel on Climate Change. IPCC, Geneva, 151 pp

Jackson CR, Meister R, Prudhomme C (2011) Modelling the effects of climate change and its uncertainty on UK Chalk groundwater resources from an ensemble of global climate model projections. J Hydrol 399:12–28

Jaunat J (2012) Caractérisation des écoulements souterrains en milieu fissuré par approche couplée hydrologie-géochimie-hydrodynamisme - application au massif de l'Ursuya (Pays Basque, France) [Characterization of groundwater flow in fissured aquifers by a multi-disciplinary approach: hydrology – geochemistry – hydrodynamics—application to the Ursuya massif (Basque-country, France)]. PhD Thesis, Université Michel de Montaigne - Bordeaux 3, Pessac, France, 344 pp

Jaunat J, Huneau F, Dupuy A, Celle-Jeanton H, Vergnaud-Ayraud V, Aquilina L, Labasque T, Le Coustumer P (2012) Hydrochemical data and groundwater dating to infer differential flowpaths through weathered profiles of a fractured aquifer. Appl Geochem 27:2053–2067

Jaunat J, Celle-Jeanton H, Huneau F, Dupuy A, Le Coustumer P (2013) Characterization of the input signal to aquifers in the French Basque Country: emphasis on parameters influencing the chemical and isotopic composition of recharge waters. J Hydrol 496:57–70

Klove B, Ala-Aho P, Bertrand G, Gurdak JJ, Kupfersberger H, Kvaerner J, Muotka T, Mykrä H, Preda E, Rossi P, Uvo CB, Velasco E, Pulido-Velazquez M (2014) Climate change impacts on groundwater and dependent ecosystems. J Hydrol 518:250–266

Koïta M, Jourde H, Rossier Y (2013) Relative importance of weathering profiles and major fracture zones to fit the water balance of a hydrogeological catchment in hard rocks. Int J Environ Sci 4:296–314

Kumar CP (2012) Climate change and its impact on groundwater resources. Int J Eng Sci 1:43–60

Kurylyk BL, MacQuarrie KT (2013) The uncertainty associated with estimating future groundwater recharge: a summary of recent research and an example from a small unconfined aquifer in a northern humid-continental climate. J Hydrol 492:244–253

Lachassagne P, Wyns R, Bérard P, Bruel T, Chéry L, Coutand T, Desprats J, Le Strat P (2001) Exploitation of high-yields in hard-rock aquifers: downscaling methodology combining GIS and multicriteria analysis to delineate field prospecting zones. Ground Water 39:568–581

Lachassagne P, Wyns R, Dewandel B (2011) The fracture permeability of hard rock aquifers is due neither to tectonics, nor to unloading, but to weathering processes. Terra Nov. 23:145–161

Landes AAL, Aquilina L, Ridder JD, Longuevergne L, Pagé C, Goderniaux P (2014) Investigating the respective impacts of groundwater exploitation and climate change on wetland extension over 150 years. J Hydrol 509:367–378

Larrasoaña JC, Parés JM, Millan H, Del Valle J, Pueyo EL (2003) Paleomagnetic, structural, and stratigraphic constraints on transverse fault kinematics during basin inversion: the Pamplona Fault (Pyrenees, north Spain). Tectonics 22:1–22

Lee J, Lee K (2000) Use of hydrologic time series data for identification of recharge mechanism in a fractured bedrock aquifer system. J Hydrol 229:190–201

Mahmoodzadeh D, Ketabchi H, Ataie-Ashtiani B, Simmons CT (2014) Conceptualization of a fresh groundwater lens influenced by climate change: a modeling study of an arid-region island in the Persian Gulf, Iran. J Hydrol 519:399–413

Maréchal J, Dewandel B, Subrahmanyam K (2004) Use of hydraulic tests at different scales to characterize fracture network properties in the weathered-fractured layer of a hard rock aquifer. Water Resour Res 40, W11508

Mattauer M, Henry J (1974) Pyrénées. Geol Soc London Spec Publ 4:3–21

Merot P, Dubreuil V, Delahaye D, Desnos P (2013) Changement climatique dans l'Ouest Évaluation, impacts, perceptions [Climate change in the west: assesment, impacts, perceptions]. Presses universitaires de Rennes, Rennes, France, 458 pp

Molina J-L, Pulido-Velazquez D, Garcia-Arostegui JL, Pulido-Velazquez M (2013) Dynamic Bayesian networks as a decision support tool for assessing climate change impacts on highly stressed groundwater systems. J Hydrol 479:113–129

Nakicénovic N, Alcamo J, Davis G, De Vries HJM, Fenhann J, Gaffin S, Gregory K, Grubler A, Jung TY, Kram T, La Rovere EL, Michaelis L, Mori S, Morita T, Papper W, Pitcher H, Price L, Riahi K, Roehrl A, Rogner H-H, Sankovski A, Schlesinger M, Shukla P, Smith S, Swart R, Van Rooijen S, Victor N, Dadi Z (2000) Special report on emissions scenarios. Intergovernmental Panel on Climate Change. Cambridge University Press, Cambridge

Neukum C, Azzam R (2012) Impact of climate change on groundwater recharge in a small catchment in the Black Forest, Germany. Hydrogeol J 20:547–560

Ondarroa C, Pesquera A, Gil PP (1998) Mineralogical and geochemical features of pegmatites from the Ursuya Massif (western Pyrenees, France). Rend Soc Ital Mineral Petrol 43:587–592

Pagé C, Terray L (2010) Nouvelles projections climatiques à échelle fine sur la France pour le 21ème siècle : les scénarii SCRATCH2010

[New climate projetions at a refine scale in France for the 21st century : the SCRATCH2010 scenarios]. CERFACS technical report TR/CMGC/10/58, CERFACS, Toulouse, France, 3 pp

Prudhomme C, Davies H (2008) Assessing uncertainties in climate change impact analyses on the river flow regimes in the UK, part 2: future climate. Clim Chang 93:197–222

Refsgaard JC, Hojberg AL, Moller I, Hansen M, Sondergaard V (2010) Groundwater modeling in integrated water resources management: visions for 2020. Ground Water 48:633–648

Serrat-Capdevila A, Valdés JB, Pérez JG, Baird K, Mata LJ, Maddock T III (2007) Modeling climate change impacts—and uncertainty—on the hydrology of a riparian system: the San Pedro Basin (Arizona/Sonora). J Hydrol 347:48–66

Shamir E, Megdal SB, Carrillo C, Castro CL, Chang H-I, Chief K, Corkhill FE, Eden S, Georgakakos KP, Nelson KM, Prietto J (2015) Climate change and water resources management in the Upper Santa Cruz River, Arizona. J Hydrol 521:18–33

Taylor R, Howard K (2000) A tectono-geomorphic model of the hydrogeology of deeply weathered crystalline rock: evidence from Uganda. Hydrogeol J 8:279–294

Taylor RG, Scanlon B, Döll P, Rodell M, van Beek R, Wada Y, Longuevergne L, Leblanc M, Famiglietti JS, Edmunds M, Konikow L, Green TR, Chen J, Taniguchi M, Bierkens MFP, MacDonald A, Fan Y, Maxwell RM, Yechieli Y, Gurdak JJ, Allen DM, Shamsudduha M, Hiscock K, Yeh PJ-F, Treidel IHH (2012) Ground water and climate change. Nat Clim Chang 3:322–329

Trefry MG, Muffels C (2007) FEFLOW: a finite-element ground water flow and transport modeling tool. Ground Water 45: 525–528

Treidel H, Martin-Bordes JJ, Gurdak JJ (2012) Climate change effects on groundwater resources: a global synthesis of findings and recommendations. IAH International Contributions to Hydrogeology. Taylor and Francis, London, 414 pp

Turner JP (1996) Switches in subduction direction and the lateral termination of mountain belts: Pyrenees-Cantabrian transition, Spain. J Geol Soc Lond 153:563–571

Virdi ML, Lee TM, Swancar A, Niswonger RG (2013) Simulating the effect of climate extremes on groundwater flow through a Lakebed. Ground Water 51:203–218

Vouillamoz J-M, Lawson FMA, Yalo N, Descloitres M (2015) Groundwater in hard rocks of Benin: regional storage and buffer capacity in the face of change. J Hydrol 520:379–386

Walker DD, Gylling B, Strom A, Selroos JO (2001) Hydrogeologic studies for nuclear-waste disposal in Sweden. Hydrogeol J 9:419–431

White A, Bullen T, Schulz M, Blum A, Huntington T, Peters N (2001) Differential rates of feldspar weathering in granitic regoliths. Geochim Cosmochim Acta 65:847–869

Wyns R, Baltassat J, Lachassagne P, Legchenko A, Vairon J, Mathieu F (2004) Application of proton magnetic resonance soundings to groundwater reserve mapping in weathered basement rocks (Brittany, France). Bull Soc Geol Fr 1:21–34

Zhou Y, Zwahlen F, Wang Y, Li Y (2010) Impact of climate change on irrigation requirements in terms of groundwater resources. Hydrogeol J 18:1571–1582